Blind prediction of broadband coherence time at basin scales

John L. Spiesberger
Department of Earth and Environmental Science, 240 South 33rd Street, University of Pennsylvania, Philadelphia, Pennsylvania 19104-6316

Frederick Tappert[a)]
Applied Marine Physics, Rosenstiel School of Marine and Atmospheric Science, University of Miami, Miami, Florida 33149

Andrew R. Jacobson
Program in Atmospheric and Oceanic Sciences, Princeton University, Princeton, New Jersey 08544-0710

(Received 28 March 2003; revised 19 September 2003; accepted 3 October 2003)

A blind comparison with data is made with a model for the coherence time of broadband sound (133 Hz, 17-Hz bandwidth) at 3709 km. Coherence time is limited by changes in the ocean because the acoustic instruments are fixed to the Earth on the bottom of the sea with time bases maintained by atomic clocks. Although the modeled coherence time depends a bit on the difficult problem of correctly modeling relative signal-to-noise ratios, normalized correlation coefficients of the broadband signals for the data (model) are 0.90 (0.83), 0.72 (0.59), and 0.51 (0.36) at lags of 2, 4.1, and 6.2 min, respectively. In all these cases, observed coherence times are a bit longer than modeled. The temporal evolution of the model is based on the linear dispersion relation for internal waves. Acoustic propagation is modeled with the parabolic approximation and the sound-speed insensitive operator. © *2003 Acoustical Society of America.* [DOI: 10.1121/1.1629305]

PACS numbers: 43.30.Re, 43.30.Zk, 43.30.Qd [RAS] Pages: 3147–3154

I. INTRODUCTION

It would be valuable to have oceanographic and acoustic models that blindly predict the broadband coherence time of sound over basin scales in the ocean. ''Blind'' means that the models are run with parameters that are taken from their expected values in the literature without any tuning to fit measurements. If such models could be constructed, they could be used to design systems, optimally process data for signals from different hypothetical locations, and serve as guides for developing theories. More specifically, reliable models for coherence time would be used by the surveillance community in the military. They would be used by ocean tomographers interested in designing sources and emitted waveforms whose receptions could gain the required signal-to-noise ratios through coherent integration. One would be able determine prior to an experiment the regimes where frequencies were sufficiently low so that propagation would be coherent for hours at a time if required. They would be used by those interested in designing and using wireless acoustic modems where one would be able to know if one could enjoy a coherent rather than incoherent communication system. As will be seen below, theories that have been applied to predict fluctuations of broadband sound at basin scales have serious discrepancies with data by one or more orders of magnitude. The existence of a reliable computational model (rather than a theory) will help guide the development of better theories. Problems with blind comparisons are useful for discovering deficiencies in models and their inputs, if any. So, for all these reasons, a blind prediction for the broadband coherence time of sound is made for a 3709-km section in the eastern North Pacific (Fig. 1) using a Monte Carlo approach. The situation is complicated by the interaction of sound with the bottom near the source and receiver. Despite these complications, it is found that the predictions for coherence time are similar to the measurements.

Blind experiments are important in most fields of science. For example, blind predictions for contemporary climate do not work[1–3] but rather need to be forced to fit current conditions. Blind clinical trials sometimes show the efficacy of a medical treatment, and sometimes do not.[4] This study may be the first blind comparison for coherence time of broadband sound over basin scales, which makes the resemblance with measurements more surprising considering the complicated nature of the transmission.

As will be seen, blind predictions for coherence time appear to be technically inconsistent with measurements at the 95%-confidence limit. Such agreement would perhaps be too much to hope for. But, the predictions are close enough to the measurements so that they appear to have utility.

One factor favoring the value of the present comparison is that the source and receiver are on the bottom. So, all the temporal changes of the signal are due to temporal changes within the ocean. Perhaps the most complicated aspect of the comparison is that the coherence time of the model depends on an accurate representation of the relative signal-to-noise ratios of the paths for each transmission. This sensitivity is small, but predictions still depend on this factor. It is possible to use the data to obtain accurate estimates of the signal-to-noise ratios, but the relative amplitudes of the model and data naturally differ on a sample-by-sample basis. Amplitudes do not obey a principle analogous to Fermat's in which travel time is insensitive to first-order changes in path. Thus,

[a)]Deceased.

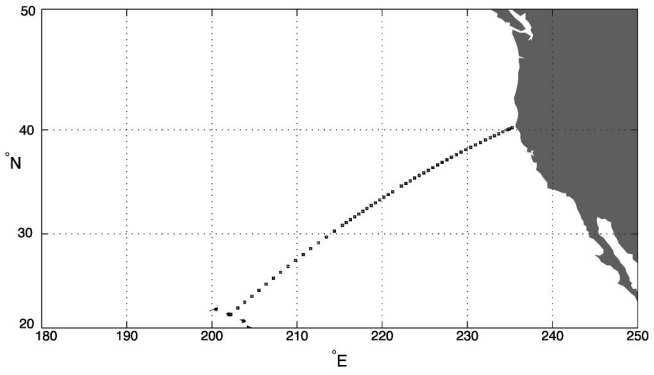

FIG. 1. Plan view of the Kaneohe source experiment. The source is located about 5 miles north of Kaneohe Bay, Oahu. The receiver near the coast of Northern California is one of many U.S. Navy SOSUS stations used to receive these transmissions. Circles indicate the positions of 56 stations where conductivity, temperature, and depth were measured with a CTD in July 1988 by the Naval Oceanographic Office.

the problem of getting the relative amplitudes right is generic to all practitioners, and is exacerbated by the fact that sound interacts with the sub-bottom where the geoacoustic properties are poorly known. Such cases deserve attention as there are so many examples where sources and receivers sit on the bottom, and predicting coherence time is valuable.

Time variability in the models is derived from the linear dispersion relation for internal waves obeying a Garrett–Munk spectrum.[5] The acoustic model is based on the parabolic approximation with the sound-speed insensitive operator.[6] It is remarkable because it appears to offer a nearly perfect solution for the travel times of broadband signals over basin scales over all launch angles without any tunable parameters.

Two studies[7,8] investigated something related to but different than coherence time of broadband sound at basin scales. In Ref. 7, the autocorrelation function is computed for travel time. The autocorrelation of a wavefront's travel time may not be sufficient to compute an integration time if phase changes of the wavefront cannot be deduced from arrival times of peaks. In other words, Ref. 7 reports an upper limit of 2 h for the *incoherent* quantity of travel time based on the amplitude (not phase) of a wavefront. Another study reports a coherent integration time of 764 s for this 3250-km transmission in the North Pacific for a source at 75 Hz and 37.5-Hz bandwidth.[9] No theory or model is used to compare with this observation.

The existing theory used in Refs. 7 and 8 to predict acoustic fluctuations may not be suitable to predict the coherence time of broadband sound. In these references, modeled energy of internal waves is adjusted so that theoretical and measured variances of travel time are the same. These reports say that the theory predicts fluctuations to be in the fully saturated regime, while instead most of the observations are reported in the unsaturated to partly saturated regimes. The reports go on to say that observations of pulse spread are two orders of magnitude different than predicted from theory. The cause for the mismatch is attributed to the fact that the theory is designed for single-frequency emissions, which the authors say is inadequate to predict broadband propagation.

The present investigation differs from those studies because acoustic data are not used here to tune a theory to fit the data, and, in fact, no theory is used. Instead, a Monte Carlo approach is used to blindly predict acoustic fluctuations with the parabolic approximation. This approximation includes the physics of finite-wavelength propagation for broadband signals. Because the prediction fits the data rather well, it appears that this and possibly other blind predictions would prove useful for improving and testing theories for the coherence time of broadband sound at long distances.

II. DATA AND MODELS

A. Data

The Kaneohe source is mounted on the bottom at 183-m depth on the north coast of Oahu at 21.512 35° N, 202.228 49° E. Continuous transmissions occur for 5 days in late 1983 to Sound Surveillance Stations (SOSUS) stations, one of which is at a distance of 3709.21 km and a depth of 1433 m near northern California at 40.078 56° N, 234.887 97° E (Fig. 1). The 183-dB *re*: 1 μPa @1 m phase-modulated signal has a center frequency of 133 Hz and a bandwidth of 17 Hz. Phase is modulated with a 511-digit maximal shift register sequence every 8 carrier cycles. The period of the signal is $511*8/133 \cong 30.7$ s. The received signal is beamformed, complex demodulated, low-pass filtered to suppress the double-frequency component, correlated with a replica to implement a matched filter, and coherently averaged over four sequence periods to boost the signal-to-noise ratio. Replica correlation compresses 30.7 s of energy along each acoustic path into a single pulse of 1/17 Hz = 0.06-s resolution without sidelobes. The output consists of records at $4 \times 30.7 \cong 123$-s intervals. Each record contains $511 \times 4 = 2044$ complex demodulates with 0.015-s separations. Atomic clocks maintain time stability at the source and receiver with a fractional frequency error of about 10^{-11}. The bathymetry in the source region is measured with an extensive SEABEAM survey.[10] Further details are discussed elsewhere.[11]

B. Model

Except for a few differences discussed below, the modeling of internal waves has been described before in detail.[12] Reference 12 includes successful comparisons of the modeling with the power spectral density of vertical displacement of water as a function of horizontal wave number, standard deviation of vertical displacement of water as a function of depth, and horizontal correlation length scale as a function of depth. A brief summary is provided here.

The sound-speed field is taken from an eddy-resolving conductivity and temperature versus depth (CTD) survey in July 1988 (Fig. 1). Most of the CTD stations extend to 2-km depth, and some to 4500 m. For comparison, the ray construction for the propagation shows lower turning depths at 2.5 km and above.[13]

The data we have do not resolve internal waves. Sound speeds below the depth of the CTD stations are taken from Levitus' climatology for spring.[14] A range-dependent three-dimensional field of internal waves is synthesized along the geodesic. Sound-speed perturbations associated with internal waves are generated by assuming that vertical displacements of water lead to adiabatic changes in the speed of sound. The acoustic propagation models described below utilize the vertical slice along the geodesic through the three-dimensional field. The internal waves have the full spectrum given by Garrett and Munk.[5] The longest horizontal wavelength represented is 80 km. The boundary conditions are zero for the vertical modes at the top and bottom; thus, the WKB approximation is not used. About 50 vertical modes are numerically computed in each 80- by 80-km horizontal region. The geodesic runs through the centers of about 50 such regions constructed by dividing the 3709-km length by the 80-km size of each region. The attendant perturbations in sound speed are smoothed at region boundaries to avoid discontinuities. Frequencies and modes of internal waves are precomputed and the linear dispersion relation is used to synthesize the field at the geophysical times desired.

Sound interacts with the bottom near the source and receiver, and this is modeled with a geoacoustic bottom.[12] Geoacoustic parameters near the receiver are modeled differently for steep and flat arriving energy, so each encounters a different reflection coefficient due to a different effective density in the sediments. Modeling the bottom in these two ways provides a way to account for the observed relative levels (Ref. 12). The geoacoustic parameters near the receiver are probably not known well enough to modify these parameters for any justifiable reason.

The requirement of this paper is to choose inputs for models that are not tuned to observations. So, instead of trying to match the relative amplitudes in the data with two different geoacoustic sets of parameters,[12] only one set of geoacoustic parameters is chosen near the receiver. The chosen geoacoustic parameters will greatly underestimate the amplitudes at the end of the reception. The same parameters near the receiver are chosen as before (Table CII, Ref. 12) except the ratio of speeds at the top of the sediment to the bottom of the water column is 1.02, and the sediment density is 1.7 kg/m^3. These parameters are chosen without regard to their effects on the model.

The sound-speed insensitive parabolic approximation[6] is used to model the propagation at each of many frequencies. An inverse Fourier transform is used to synthesize the broadband impulse response. That response is complex demodulated to produce samples at 0.0152-s intervals. This is similar to the data interval. A running average of 4 complex demodulates is then used to mimic the matched filter for the data. The computational grid[12] is small enough to yield convergence within a few decibels at the receiver. The parabolic approximation includes acoustic absorption that depends on frequency in the standard way.

Models are synthesized from realizations of the internal wave field at 123-s intervals over a geophysical time of 3.4 and 2 h, respectively, for normal and half-normal energy of the Garrett–Munk spectrum.[5] Thus, there are 100 and 59 realizations, respectively, for the normal and half-normal runs. Each realization requires 5 h on an AMD Athlon 1800+ processor, so all model realizations require 795 h. Fifty-nine realizations at the half-normal level appear to be sufficient to examine the sensitivity of the model predictions.

III. RESULTS

A. Incoherent averages

The long-term stability or instability of features in the data can often be investigated by averaging the receptions during long periods of time. If the data were phase coherent for many hours at a time, one would naturally coherently average the complex records together, and look for stable features between separate averaging periods. Since the data in this experiment are not phase coherent over periods like hours, the stability of features can be investigated using an incoherent average, i.e., an average that discards acoustic phase. The incoherent average is one way to form this average. Averages are made over intensity, and then a square root can be taken to yield an amplitude scale.

The incoherent average for the mth demodulate, $a[m]$, is formed from N_{rec} records as

$$a[m]=\left[\frac{1}{N_{\mathrm{rec}}}\sum_{r=1}^{N_{\mathrm{rec}}}\frac{\|d[m,r]\|^2}{\sigma[r]^2}\right]^{1/2},\quad m=1,2,\ldots,M, \tag{1}$$

where the mth complex demodulate of the rth record is $d[m,r]$. Note that $a[m]$ is a measure of the expected value of a dimensionless amplitude of $d[m,r]$ because $d[m,r]$ is divided by its standard deviation. The variance of the noise for record r is $\sigma[r]^2$, and is included to give proper weight to records based on their signal-to-noise ratios. When forming incoherent averages from data, $\sigma[r]^2$ is estimated from each data record where signal is not present. This is easy to do because each record consists of about 30.7 s of complex demodulates, only 4 s of which cover the time that the energy is present in significant quantity.[11] When forming incoherent averages from model realizations, $\sigma[r]^2$ is set to unity.

Noise is added to each model record in the following way prior to forming the incoherent average. The average signal-to-noise ratio in the data is not stationary from one record to the next. For data record i, the average signal-to-noise is estimated between the travel times of 2504.2 to 2505.2 s. Then, 5 s of noise from the data are taken from record i, and added to the ith model realization with the same signal-to-noise ratio as the modeled travel times from 2504.2 and 2505.2 s.

An addition of 0.367 s to modeled travel times aligns them with the data on 29 Nov. 1983 (Fig. 2). Rossby waves are likely responsible[15] for some of the 0.367 s. In order to achieve a match between the duration of the energy between model and data, a previous investigation finds it necessary to add internal wave and mesoscale components to the climatological averages of sound speed.[12] It appears that the model duration in Fig. 2 is similar to the data, but the model amplitudes are too low at the end near 2507.5 s, just like that found before for similar values of geoacoustic parameters near the receiver.[12] If two models are used with different sets

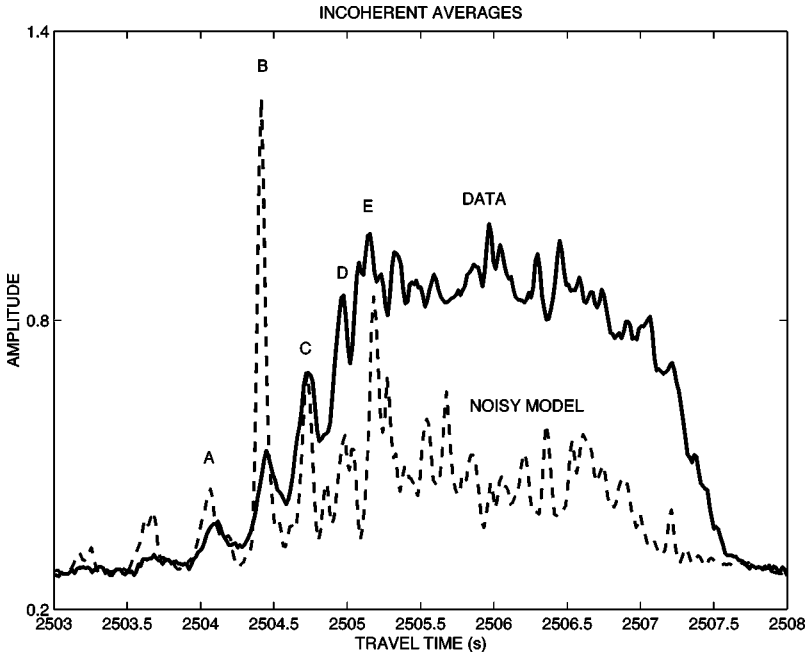

FIG. 2. Incoherent averages for the data at Northern California on 29 Nov. 1983 (Fig. 1) compared with an incoherent average of model realizations. Paths A–E can be tracked throughout the intermittent transmissions covering 6 years, 1983–1989. The time evolution of the modeled sound-speed field is determined by the linear dispersion relation of internal waves used by Garrett and Munk (Ref. 5). Modeled internal waves are superimposed on the mesoscale resolving CTD section (Fig. 1). The incoherent average of the data consists of 703 records at 123-s intervals, which covers a day. The incoherent average from the model consists 100 runs separated by 123 s each, which is a duration of 3.4 h, 0.367 s is added to modeled travel times to align with the data. Rossby waves are probably responsible for some of the 0.367 s (Ref. 15).

of geoacoustic parameters for flat and steeply arriving energy, amplitudes better resemble the observations.[12]

Even if two sets of geoacoustic parameters are used to better predict amplitudes, there are still differences between model and data. Four possibilities for this difference are listed. First, the models only cover 3.4 h of geophysical time, and the data cover a day. Second, the daily incoherent averages of the data are not stationary (Fig. 3 in Ref. 13). Third, the geoacoustic parameters for the bottom are imperfect. Fourth, the sound-speed field for the model is imperfect. A further discussion of amplitude differences is beyond the scope of this paper.

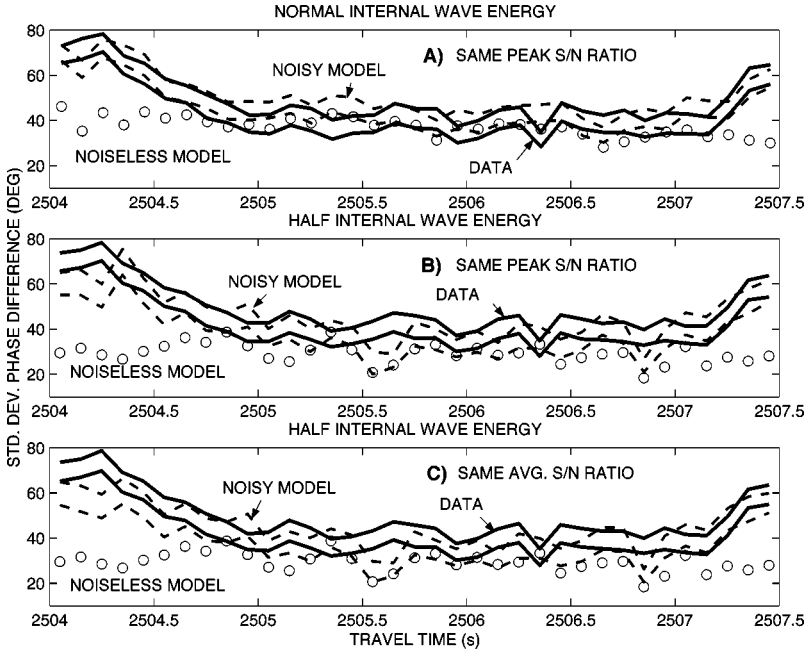

FIG. 3. The 95%-confidence limits, via the bootstrap (Ref. 16), for the standard deviation of change in acoustic phase at 123-s intervals across a 3709-km section (Fig. 1) for the data, noiseless, and noisy models. The standard deviation is estimated in 35 windows of 0.1-s duration each between 2504 and 2507.5 s of travel time. The comparison is made using data records starting at 1 Dec. 1983 18:13:12 (GMT). The model is the sound-speed insensitive parabolic approximation (Ref. 6). The sound-speed field has a mesoscale (Fig. 1) and a time-evolving internal wave field based on the linear dispersion relation for internal waves. (A) The model uses the normal Garrett–Munk (Ref. 5) energy spectrum where the peak signal-to-noise ratio in each data window sets the peak signal-to-noise ratio in each model window. Models are generated from 100 realizations of internal waves at 123-s intervals. Models are compared to 100 consecutive data records. (B). Same as (A) except the model has one-half the Garrett–Munk energy level and uses 59 realizations of the internal wave field at 123-s intervals. The models are compared to 59 consecutive data records. (C) Same as (B) except the signal-to-noise ratio of the average of the five largest intensities in each 0.1-s data window sets the signal-to-noise ratio of the five largest intensities in each model window. Model results are given with and without acoustic noise. The 95% limits are not given for the noiseless model.

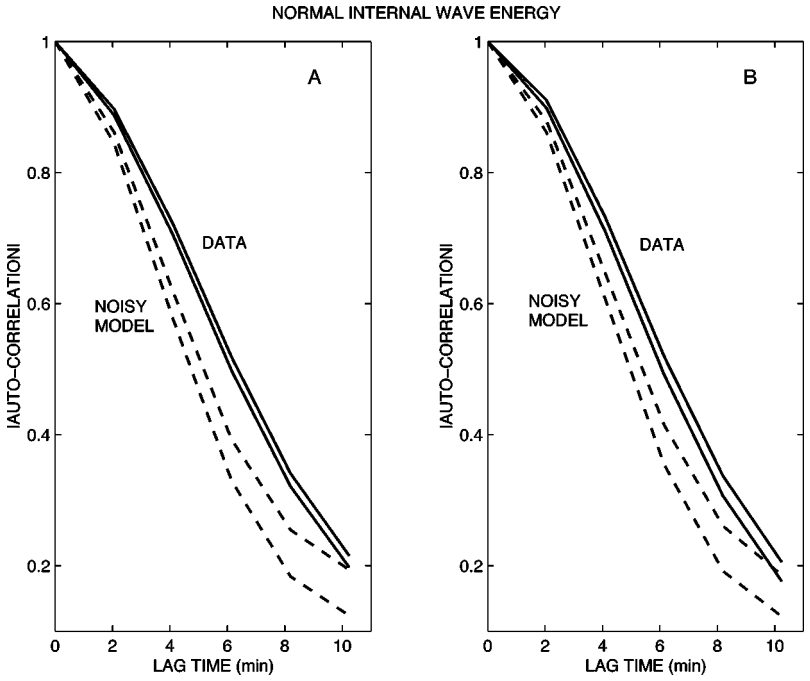

FIG. 4. Coherence time via Eq. (2) of the data and models with 95% confidence limits computed via the bootstrap (Ref. 16). The 95%-confidence limits are indicated by two curves for the data and two curves for the model. An average signal-to-noise ratio in each data record is used to set the same in each model record to produce the ''noisy model'' results. The comparisons are made with normal energy in the Garrett–Munk spectrum of internal waves using the linear dispersion relation of these waves to evolve the fields at 123-s intervals for 100 model realizations. The model realizations are compared with 100 consecutive data records. (A) Coherence time for energy between 2504 and 2507.5 s (Fig. 2). (B) Same but for energy between 2505.5 and 2506.6 s.

B. Phase differences

Differences in acoustic phase between adjacent records at the same travel time are estimated by first unwrapping phases by choosing the angle closest to the prior one, and then taking the difference in angle between the unwrapped phases. The largest value for the standard deviation of these differences is given by the standard deviation of a uniformly distributed random variable on the interval $[0,2\pi]$ which is $\sqrt{(2\pi)^2/12}$ radians or 104 deg. The standard deviation of the phase differences is plotted (Fig. 3) for travel times between 2504 and 2507.5 s because this is when the signal arrives (Fig. 2).

Depending on the precise time window used for computation of the Fourier transform of the time series, the scintillation index has values between 0.8 to 1.4 at 133 Hz. Phase differences for noisy models are about 20 to 40 deg larger than noiseless models at travel times near 2504 and 2507.5 s because the signal-to-noise ratio is small (Fig. 3). As the signal-to-noise ratio rises, the differences between noiseless and noisy models decreases to 5 to 10 deg. The standard deviation of phase difference is not a strong function of travel time in the noiseless model case or in the data, except for the data when the signal-to-noise ratio is lower near 2504 and 2507.5 s. The standard deviations of phase differences are significantly less than 104 deg, which would be that due to independently distributed uniform random noise. We conclude that a blind comparison between model and data yields statistically compatible results for most of the record.

Turning to a nonblind prediction, it is found that halving the energy in the Garrett–Munk spectrum of internal waves tends to decrease the standard deviations by about 10 deg in the noiseless models (panels A and B, Fig. 3). The standard deviations of the noisy models decrease in places by perhaps 10 deg, but the change is smaller because noise is not allowing the standard deviations to decrease as much as that from the effects of reducing the energy in the internal waves.

The standard deviation of the noisy model decreases by about 5 deg or less when the average rather than peak signal-to-noise ratio is imposed on the model (panels B and C, Fig. 3) at the one-half energy level for internal waves. Given the sensitivities of the comparison to the manner in which noise is added to the model, it does not appear to be productive to use further analysis to determine which energy level gives the best fit with the data.

C. Coherence time

Coherence time (Fig. 4) is estimated using an autocorrelation function

$$A(p)=\left|\frac{\Sigma_{r=1}^{R}\Sigma_{m=1}^{M}d[m,r]d^{*}[m,r+p]}{\Sigma_{r=1}^{R}\Sigma_{m=1}^{M}d[m,r]d^{*}[m,r]}\right|, \tag{2}$$

where the superscript * denotes complex conjugate, and the vertical bars denote the modulus of the complex number. 95% confidence limits for $A(p)$ are estimated using the bootstrap.[16] The 95%-confidence limits are indicated in Fig. (4) by two curves for the data and two curves for the model. R pairs of records are used for the estimate and M complex demodulates are used for two windows of arrival time. The first is from 2504 to 2507.5 s, which encompasses most of the energy (Fig. 2). The second is from 2505.5 to 2506.5 s, a region where the signal-to-noise ratios are high and the relative amplitudes in the data and model are relatively flat. In both cases, an average of the largest N intensities in the data in each record is used to estimate an average intensity signal-to-noise ratio to set the same in the model. N is 200 and 50 for the wider and narrower windows, respectively. A smaller value of 50 is used for the latter because that window contains only 66 samples. Correlation values in Fig. 4 drop by amounts of between 0 and 0.3 for the noisy model if the peak signal-to-noise ratio in each data window is used to set the peak signal-to-noise ratio in each model window on a record-

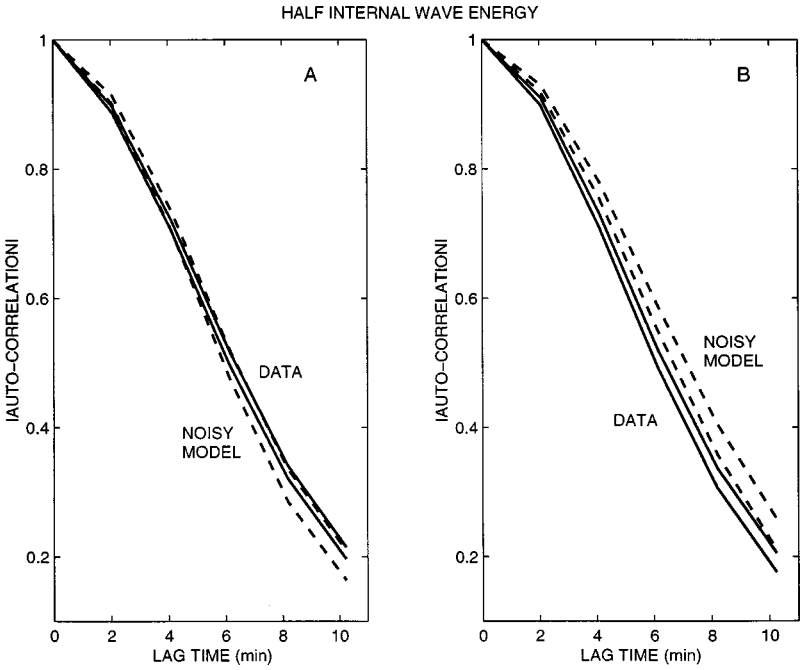

FIG. 5. Same as Fig. 4 except for half-normal energy in the Garrett–Munk field of internal waves (Ref. 5). In this case, 59 model realizations are compared with 59 data records.

by-record basis. Evidently, specifying the model's signal-to-noise ratio from the highest peak in the data results in an overall smaller signal-to-noise ratio in the model than setting the model's signal-to-noise ratio according to the highest N intensities in the data.

Figure 4 represents a blind comparison of model with data. Because some of the literature[7,8] discusses the possibility that a half-normal energy of internal waves may better fit observations, a prediction based on this lower energy is made here (Fig. 5). This is not a blind comparison because the expected energy level for internal waves is not used. The noisy model looks like observed coherence times for the longer data window, but not for the shorter one.

IV. BATHYMETRY AND GEOACOUSTIC BOTTOM: EFFECTS ON COHERENCE TIME

One might wonder whether the rather close agreement between modeled and observed coherence time is fortuitous. Lines of reasoning based on the modeling and data support the conclusion that the agreement is not fortuitous. In time, however, the strongest test for the validity of a new scientific finding or approach involves many scientists who apply the technique to many different experiments and obtain similar results.

The fact that the blind modeling yields an answer close to observed coherence times seems to be a reason to believe that the agreement is not fortuitous. There are many ways the modeling could have gone astray. Acoustic models that do not couple modes or that do not yield accurate travel times for a wide range of acoustic launch angles would seem to yield highly inaccurate impulse responses. Indeed, the sound-speed insensitive parabolic approximation,[6] the bathymetry, and geoacoustic parameters yield a good match to the impulse response.[12,13] The bathymetry was carefully measured by SEABEAM near the source and by the Navy near the receiver. The set of geoacoustic parameters used here is selected from the best available unclassified values in the literature.[12] There are undoubtedly bathymetric profiles and geoacoustic parameters that would not yield a good match with the data. It is often difficult to get a model to agree with observations without tuning or fitting.[1–3] The fact that the modeled impulse response looks like the data indicates that the models have the acoustic paths about right, and lends evidence to support that the bathymetry and geoacoustic parameters are reasonable.

Going further, let us continue to hypothesize that uncertainties in bathymetry or in the geoacoustic parameters lead to significant changes in predicted coherence time. In other words, one is invoking a time-independent process to explain changes in a time-dependent phenomenon. The only thing in the modeling that has time dependence is the evolving internal wave field. If the internal waves are frozen, then one obtains an infinite coherence time at the receiver. Let us see where the turning on of ocean fluctuations leads us, taking into account the observations. Much of the discussion that follows has appeared before.[10]

The only way this time-independent phenomenon can affect this time-dependent phenomenon is if temporal fluctuations in the water column lead to significant changes in the acoustic travel times by changing the *paths* by which sound travels. The evidence against significant changes in path is significant for the following reasons.

First, changes in travel time due to changes in path are guaranteed to be of second-order importance because of Fermat's principle. The zero-order change in travel time is an integral of the fluctuations of sound speed due to internal waves along a frozen ray path. The first-order change is due to changes in path due to those fluctuations, which is zero because of Fermat's principle. The second-order change is due to changes in path. Fermat's principle thus supports the notion that modeled coherence time is insensitive to plausible changes in the geoacoustic parameters with respect to the set of values used in this paper.

Second, sound interacts with the bottom and sub-bottom with different angles of incidence in this experiment at both the source and receiver. This means that the sonic paths themselves sense different effective bathymetric and geoacoustic values, and all the sonic energy interacts with the bottom in this experiment.[12] The evidence in this paper (Figs. 3, 4) demonstrates that the coherence time of sound is not sensitive to which acoustic energy is being analyzed. This means that actual different bathymetric and geoacoustic values that are important for the different paths are not important in changing their coherence times. Thus, the data themselves provide a sensitivity analysis that points to a lack of sensitivity in the calculations for coherence time.

Third, experimental evidence supports the hypothesis that any changes in path geometries lead to small changes in travel time. The travel times of the peaks of the five stable arrivals all change by the same amount at the same time by up to 1/2 second, within measurement error.[10] If these paths change significantly, it is hard to see why their travel time changes would be the same since the points at which they reflect from the bottom are all different from one another, and it would be expected that their travel times would thus change in a discordant manner.

Fourth, evidence based on detecting small tidal signals suggests that any path changes lead to very small changes in travel time. The barotropic and internal tides generated by flat-topped seamounts several thousands of kilometers from the source can be accurately estimated at five SOSUS stations, despite the fact that the tidal signals amount to only about 10 ms of travel time. The time series of these 10-ms tidal oscillations are very clean, showing little evidence of noise. The ability to detect the small signals is due to the use of the phase and amplitude of the acoustic signals. Indeed, the measurements are made with an accuracy of 135 μs at 2-min intervals over several months.[10]

These lines of reasoning support a conclusion that the agreement between modeled and observed coherence time is not sensitive to plausible changes in the bathymetry and the geoacoustic values in this experiment.

V. CONCLUSIONS

Blind predictions for the coherence times of broadband signals at basin scales are similar to but a little less than observed (Fig. 4). The blind prediction utilizes the the Garrett–Munk spectrum of internal waves[5] and a sound-speed insensitive parabolic approximation.[6] A blind prediction for the standard deviations of broadband phase differences at 2-min intervals is statistically consistent with observations (Fig. 3). The results above depend somewhat, but not much, on the method used to assign a signal-to-noise ratio to each complex sample from the model.

Despite the fact that the overall relative amplitudes in the model and data differ, especially near the coda, the predictions for coherence time do not change much (e.g., panels A and B in Fig. 4) when different windows in arrival time are used for the blind comparison. This is fortunate because it is usually difficult for practitioners to model amplitudes for sources and receivers on the bottom. The difficulty in getting the relative amplitudes right probably comes from the lack of accurate geophysical parameters for the sub-bottom, limited ways that the acoustic model can incorporate those parameters, a lack of a stability principle for amplitudes, and the fact that the ocean's change from day-to-day leads to changes in the relative amplitudes of the paths (Fig. 3, Ref. 13).

Departing from a blind prediction, a nonblind prediction is made for internal waves at one-half normal energy. The comparison with the standard deviation of phase at 2-min intervals agrees with the data at both half and normal energy (Fig. 3). The comparison with coherence time agrees with the data for one data window and disagrees with another data window (Fig. 5). We believe that the analysis in this paper is insufficient to decide if the half-normal energy better fits the data than the case with normal energy. In order to decide this issue, we would feel more comfortable if there were more degrees of freedom from which to make comparisons. For example, it would be desirable to have a month of continuous results from models and data.

Considering the discrepancies between blind predictions and observations in some fields such as the study of the Earth's climate,[1–3] it is remarkable that blind predictions for sound comes so close to reality. It is worthwhile to try blind predictions for different experiments.

ACKNOWLEDGMENTS

This research was supported by the Office of Naval Research Contract No. N00014-00-C-0317. John Spiesberger thanks Bruce Einfalt for programming expertise and Michael Wolfson for previous collaborative research during which some of the computer software used here was developed. We thank the reviewers for catalyzing the perspective of how the results in this paper fit into the field of sound transmission in the ocean and for questions which led us to improve its quality, including the addition of Sec. IV.

[1] S. Manabe, R. J. Stouffer, M. J. Spelman, and K. Bryan, "Transient responses of a coupled ocean–atmosphere model to gradual changes of atmospheric CO_2. I. Annual mean response," J. Clim. **4**, No. 8, 785–818 (1991).

[2] S. Manabe and R. J. Stouffer, "Century-scale effects of increased atmospheric CO_2 on the ocean–atmosphere system," Nature (London) **364**, 215–218 (1993).

[3] J. T. Houghton, Y. Ding, D. J. Griggs, M. Noguer, P. J. van der Linden, X. Dai, K. Maskell, and C. A. Johnson, "Climate Change 2001: The Scientific Basis," Contribution of Working Group I to the *Third Assessment Report of the Intergovernmental Panel on Climate Change* (IPCC) (Cambridge University Press, Cambridge, 2001).

[4] *Fundamentals of Clinical Trials*, 3rd ed., edited by L. M. Friedman, C. D. Furberg, and D. L. DeMets (Springer, New York, 1998).

[5] C. Garrett and W. Munk, "Space-time scales of internal waves," Geophys. Fluid Dyn. **2**, 225–264 (1972).

[6] F. Tappert, J. L. Spiesberger, and L. Boden, "New full-wave approximation for ocean acoustic travel time predictions," J. Acoust. Soc. Am. **97**, 2771–2782 (1995).

[7] J. A. Colosi, E. K. Scheer, S. M. Flatte, B. D. Cornuelle, M. A. Dzieciuch, W. H. Munk, P. F. Worcester, B. M. Howe, J. A. Mercer, R. C. Spindel, K. Metzger, T. G. Birdsall, and A. B. Baggeroer, "Comparisons of measured and predicted acoustic fluctuations for a 3250-km propagation experiment in the eastern North Pacific Ocean," J. Acoust. Soc. Am. **105**, 3202–3218 (1999).

[8] S. M. Flatte, J. A. Colosi, M. A. Dzieciuch, and P. F. Worcester, "Acoustic observations of internal-wave strength in the Mid-Pacific in 1989 and 1996," J. Acoust. Soc. Am. **100**, 2582 (1996).

[9] P. F. Worcester, B. D. Cornuelle, M. A. Dzieciuch, W. H. Munk, B. M. Howe, J. A. Mercer, R. C. Spindel, J. A. Colosi, K. Metzger, T. G. Birdsall, and A. B. Baggeroer, ''A test of basin-scale acoustic thermometry using a large-aperture vertical array at 3250-km range in the eastern North Pacific Ocean,'' J. Acoust. Soc. Am. **105**, 3185–3201 (1999).
[10] J. L. Spiesberger, ''An updated perspective on basin-scale tomography,'' J. Acoust. Soc. Am. **109**, 1740–1742 (2001).
[11] J. L. Spiesberger, P. B. Bushong, K. Metzger, and T. G. Birdsall, ''Ocean acoustic tomography: Estimating the acoustic travel time with phase,'' IEEE J. Ocean. Eng. **14**, 108–119 (1989).
[12] M. A. Wolfson and J. L. Spiesberger, ''Full wave simulation of the forward scattering of sound in a structured ocean: A comparison with observations,'' J. Acoust. Soc. Am. **106**, 1293–1306 (1999).
[13] J. L. Spiesberger and F. D. Tappert, ''Kaneohe acoustic thermometer further validated with rays over 3700 km and the demise of the idea of axially trapped energy,'' J. Acoust. Soc. Am. **99**, 173–184 (1996).
[14] S. Levitus, ''Climatological atlas of the world ocean,'' in *NOAA Professional Paper 13* (U.S. Government Printing Office, Washington, DC, 1982).
[15] J. L. Spiesberger, H. E. Hurlburt, M. Johnson, M. Keller, S. Meyers, and J. J. O'Brien, ''Acoustic thermometry data compared with two ocean models: The importance of Rossby waves and ENSO in modifying the ocean interior,'' Dyn. Atmos. Oceans **26**, 209–240 (1998).
[16] B. Efron and R. J. Tibshirani, *An Introduction to the Bootstrap* (Chapman and Hall, New York, 1993).